

Original Article

Kir4.1 is coexpressed with stemness markers in activated astrocytes in the injured brain and a Kir4.1 inhibitor BaCl₂ negatively regulates neurosphere formation in culture

Jae-Kyung Kwon¹, Dong-Joo Choi^{2,3}, Haijie Yang^{1,2,4}, Dong Wan Ko^{1,2}, Ilo Jou^{1,2,3}, Sang Myun Park^{1,2,3}, and Eun-Hye Joe^{1,2,3,4,5,*}

¹Neuroscience Graduate Program, Department of Biomedical Sciences, ²Department of Pharmacology, ³Chronic Inflammatory Disease Research Center, ⁴Center for Convergence Research of Neurological Disorders, ⁵Department of Brain Science, Ajou University School of Medicine, Suwon 16499, Korea

ARTICLE INFO

Received May 9, 2021
Revised August 10, 2021
Accepted September 7, 2021

*Correspondence

Eun-Hye Joe
E-mail: ehjoe@ajou.ac.kr

Key Words

Kir4.1
Reactive astrocyte
Sox2
Stem cells

ABSTRACT Astrocytes are activated in response to brain damage. Here, we found that expression of Kir4.1, a major potassium channel in astrocytes, is increased in activated astrocytes in the injured brain together with upregulation of the neural stem cell markers, Sox2 and Nestin. Expression of Kir4.1 was also increased together with that of Nestin and Sox2 in neurospheres formed from dissociated P7 mouse brains. Using the Kir4.1 blocker BaCl₂ to determine whether Kir4.1 is involved in acquisition of stemness, we found that inhibition of Kir4.1 activity caused a concentration-dependent increase in sphere size and Sox2 levels, but had little effect on Nestin levels. Moreover, induction of differentiation of cultured neural stem cells by withdrawing epidermal growth factor and fibroblast growth factor from the culture medium caused a sharp initial increase in Kir4.1 expression followed by a decrease, whereas Sox2 and Nestin levels continuously decreased. Inhibition of Kir4.1 had no effect on expression levels of Sox2 or Nestin, or the astrocyte and neuron markers glial fibrillary acidic protein and β -tubulin III, respectively. Taken together, these results indicate that Kir4.1 may control gain of stemness but not differentiation of stem cells.

INTRODUCTION

Astrocytes, the most abundant cells in the brain, play a role in supporting brain functions. In particular, astrocytes remove extracellular potassium (K⁺) and neurotransmitters released from neurons during action potential generation, thereby allowing continuous neural conduction.

Kir4.1, an inward-rectifier K⁺ channel that is highly expressed in astrocytes, is involved in maintaining extracellular K⁺ ions at synaptic sites [1-3]. In addition to maintenance of K⁺ homeostasis, Kir4.1, together with aquaporin 4, regulates astrocyte volume [4]. Kir4.1 is also functionally coupled with the glutamate transporters, glutamate transporter-1 (GLT-1) and glutamate aspartate

transporter (GLAST) [5]. Accordingly, defects in astrocytic Kir4.1 channels could contribute to diverse brain diseases, including Huntington's disease, multiple sclerosis, and depression [6-8]. Kir4.1 may regulate the proliferation of cells in addition to maintaining extracellular neurotransmitters and ions since regulation of intracellular K⁺ ions changes membrane potential, which is an important factor in modulation of cell-cycle progression [9,10].

Astrocytes are activated in the injured brain [11,12]. The resulting reactive astrocytes show increased expression levels of cytoskeletal proteins, glial fibrillary acidic protein (GFAP) and vimentin; become hypertrophic with thicker and longer processes [11,12]; and proliferate [13]. It has been reported that reactive astrocyte may be involved in neurogenesis through conversion to



This is an Open Access article distributed under the terms of the Creative Commons Attribution Non-Commercial License, which permits unrestricted non-commercial use, distribution, and reproduction in any medium, provided the original work is properly cited. Copyright © Korean J Physiol Pharmacol, pISSN 1226-4512, eISSN 2093-3827

Author contributions: J.K.K. performed most of the experiments, analyzed the results, and wrote the article. D.J.C., H.Y., and D.W.K. provided technical assistance with animal studies and analyzed the results. I.J. and S.M.P. discussed the experiments regarding the roles of astrogliosis. E.H.J. conceived the idea for the project, analyzed the results, and wrote the article. All authors reviewed the results and approved the manuscript.

neurons [14-16]. Consistent with this, reactive astrocytes around injury sites have been shown to possess stem cell-like properties similar to those of neural precursor cells, including self-renewal and multipotency [17-19]. These properties of reactive astrocytes are accompanied by an increase in the expression of Sox2 (sex determining region of Y chromosome [Sry]-related high mobility group box2), a transcription factor expressed in neural stem cells that serves as a marker of these cells [20]. Sox2 expression is maintained at low levels in the intact brain, but is increased in the injured brain [21]. Sox2 may be critical for injury-induced proliferation of astrocytes, as evidenced by the fact that Sox2 deletion decreases astrocyte proliferation [21]. Accordingly, reactive astrocytes gain properties of neural stem cells (NSCs) after traumatic or ischemic brain injury. Specifically, when cultured in the presence of epidermal growth factor (EGF) and fibroblast growth factor (FGF), astrocytes obtained 3–5 days after such brain injuries form spheres and display multipotency, exhibiting the capacity to differentiate into all three types of brain cells: neurons, oligodendrocytes, and astrocytes [17,19].

In this study, we found that Kir4.1 expression in Sox2- and Nestin-positive reactive astrocytes obtained following brain injury was increased near the injury core. In cultured neural stem cells, inhibition of Kir4.1 channels with the selective inhibitor BaCl₂ increased expression of Sox2 and increased the size of neurospheres. Thus, Kir4.1 may exert negative effects on sphere formation by suppressing excessive increases in Sox2 expression.

METHODS

Animals

C57BL/6 mice (male, 8–10 w, 20–25 g) were housed under a 12 h light/dark cycle with free access to food and water. All experiments were performed in accordance with approved animal protocols and guidelines established by the Ajou University School of Medicine Ethics Review Committee (2014-0029, AMC119).

Stereotaxic injection

Mice were anesthetized with intraperitoneal injections of tribromoethanol (250 mg/kg; Sigma-Aldrich, St. Louis, MO, USA), and placed in a stereotaxic apparatus (David Kopf Instruments, Tujunga, CA, USA). Brain injury was produced by unilateral administration of ATP (500 mM, 0.8 µl; Sigma-Aldrich), a component of DAMPs produced in pathological conditions [22-25], into the striatum (from bregma: AP, +1.0 mm; ML, -1.9 mm; DV, -3.2 mm), according to stereotaxic coordinates in The Atlas of the Mouse Brain (Paxinos and Franklin, second edition), as previously described [26]. ATP was injected at a rate of 0.2 µl/min using a Hamilton syringe equipped with a 33-gauge needle attached to a syringe pump (KD Scientific, New Hope, PA, USA); the needle

was left in place for an additional 10 min prior to removal to prevent leakage through the needle track.

Sphere culture from neonatal brains

Mice at postnatal day 7 (P7) were anesthetized, and cortical slices (400 µm thick) were prepared using a McIlwain tissue chopper (Mickle Laboratory Engineering, Goose Green, UK). Slices are immediately collected and incubated in Accumax (Millipore, Bedford, MA, USA) for 15 min at 37°C. Lysed tissues are homogenized into a single-cell suspension in culture medium by trituration with a flame-polished Pasteur pipette. Cells were resuspended in Dulbecco's Modified Eagle's Medium/Nutrient Mixture F-12 (DMEM/F12; WelGene, Daegu, Korea) containing 0.9 M sucrose and centrifuged to remove myelin (111 ×g for 10 min). Cells were grown in a 100-mm Petri dish with NSC growth medium (DMEM/F12) containing N-2, B27 supplement without vitamin A (Gibco-Invitrogen, Carlsbad, CA, USA) together with EGF and bFGF (20 ng/ml each; BD Bioscience, San Jose, CA, USA). For Kir4.1-inhibition experiments, cells were treated with 1 µg/ml BaCl₂ (Sigma-Aldrich) after 3 h. The size of neurospheres was measured after 1, 3, and 5 d. For differentiation, cells were collected and incubated in Accumax for 5 min. After centrifugation (180 ×g, 3 min), dissociated cells were seeded on plates coated with 0.2 mg/ml poly-L-ornithine and 1 µg/ml fibronectin (Sigma-Aldrich) in the absence of growth factors.

Primary neural stem cell culture

Forebrains from embryonic day 13.5 (E13.5) mice were freed of meninges and gently triturated several times in culture medium using a flame-polished Pasteur pipette. Cells from a brain were plated in a 100-mm Petri dish and cultured in DMEM/F12 medium supplemented with N-2 and B27 supplement without vitamin A. EGF and bFGF (20 ng/ml each) were added every 2 d. For differentiation, dissociated cells were seeded on plates coated with 0.2 mg/ml poly-L-ornithine and 1 µg/ml fibronectin in the absence of growth factors. Cells were treated with 1 µg/ml BaCl₂ 3 h after seeding.

Western blotting

Cells and mouse brains were lysed on ice in RIPA buffer (10 mM sodium phosphate buffer pH 7.2, 150 mM NaCl, 1% NP-40, 0.5% sodium-deoxycholate) containing phosphate/protease inhibitor cocktails (GenDEPOT, Barker, TX, USA). Proteins were separated by SDS-PAGE, transferred to nitrocellulose membranes, and identified by incubating membranes with specific primary antibodies (Table 1) overnight at 4°C. After washing with phosphate-buffered saline (PBS), membranes were incubated with peroxidase-conjugated secondary antibodies and visualized using an enhanced chemiluminescence system (Daeil Lab Inc.,

Seoul, Korea). Band intensities were normalized to β -actin or glyceraldehyde-3-phosphate dehydrogenase (GAPDH) using Image J.

Immunohistochemistry

Mice were anesthetized and transcardially perfused first with saline solution containing 0.5% sodium nitrate and heparin (10 unit/ml) and then with 4% paraformaldehyde in 0.1 M phosphate buffer (pH 7.4). Brains were obtained and post-fixed overnight at 4°C with 4% paraformaldehyde. Fixed brains were stored at 4°C in a 30% sucrose solution until they sank. Series of coronal sections (30 μ m thick) were obtained with a cryostat (Leica, Wetzlar, Germany) and used for immunohistochemistry.

For 3,3'-diaminobenzidine staining, brain sections were rinsed three times with PBS, treated with 3% H₂O₂ for 5 min, and rinsed with PBS containing 0.2% Triton X-100 (PBST). After blocking non-specific binding with 1% bovine serum albumen (BSA) in PBST, sections were incubated overnight at room temperature with primary antibodies (Table 1). Sections were rinsed with PBST and incubated with biotinylated secondary antibodies (Vector Laboratories, Burlingame, CA, USA), then mounted on gelatin-coated slides and examined under a bright field microscope (BX51; Olympus Optical, Tokyo, Japan). For immunofluorescence staining, brain sections were fixed with 4% paraformal-

dehyde at room temperature for 20 min, washed with PBS, and incubated in in PBS containing 1% BSA and 0.1% Triton X-100 for 30 min. Sections were then incubated overnight with primary antibodies (Table 1) at 4°C, washed with PBS, and incubated with fluorescence-conjugated secondary antibodies (Gibco-Invitrogen) for 2 h. Finally, sections were washed, mounted using a mounting medium containing 4',6-diamidino-2-phenylindole (DAPI; Vector Laboratories) and examined under a ZEISS LSM 800 confocal laser-scanning microscope (Carl Zeiss, Göttingen, Germany).

Real-time PCR

Total RNA was isolated from primary astrocytes using easy-BLUE reagent (iNtRON Biotechnology, Seoul, Korea). cDNA was synthesized from 1 μ g of total RNA using a cDNA synthesis kit (iNtRON Biotechnology) under the following incubation conditions: denaturation at 75°C for 5 min, cDNA synthesis at 42°C for 60 min, and termination at 70°C for 5 min. Quantitative polymerase chain reaction (qPCR) was performed using 2x KAPA SYBR Fast Master Mix (Kapa Biosystems, Cape Town, South Africa) and an RG-6000 real-time amplification instrument (Corbett Research, Sydney, Australia). Primers for qPCR are listed in Table 2. The cycle threshold (Ct) for a given gene transcript was normalized to the average Ct for transcripts of the housekeeping gene, GAPDH. Relative quantitation of normalized transcript abundance was determined using the comparative Ct ($\Delta\Delta$ Ct) method.

Statistical analysis

Statistical analysis was performed using the GraphPad Prism software (Prism; San Diego, CA, USA). Data were analyzed using two tailed, unpaired t-test for comparison of two groups. Two-way analysis of variance (ANOVA) was applied for comparison of multiple groups. The p-values are also indicated in the figure legends. All values are means \pm SEMs of at least three independent experiments.

Table 1. Primary antibody

Antibody	Company	Dilution
Sox2	Santa Cruz Biotechnology, Dallas, TX, USA	1:1,000 (WB)
Nestin	Millipore, Bedford, MA, USA	1:1,000 (WB)/ 1:200 (IHC, ICC)
GFAP	SIGMA-ALDRICH, St.Louis, MO, USA	1:5,000 (WB)
GFAP	Custom	1:1,000 (IHC)
Kir4.1	Alomone Labs, Jerusalem, Israel	1:2,000 (WB)/ 1:100 (IHC, ICC)
Tuj-1	Abcam, Cambridge, UK	1:1,000 (WB)
GAPDH	Cell Signaling Technology, Danvers, MA, USA	1:5,000 (WB)

GFAP, glial fibrillary acidic protein; IHC, immunohistochemistry; ICC, immunocytochemistry; WB, Western blotting.

Table 2. qPCR primers

Primer	Sense	Anti-sense
Sox2	5'- GGC AGC TAC AGC ATG ATG CAG	5'- CTG GTC ATG GAG TTG TAC TGC
GFAP	5'- AGC TAG CCC TGG ACA TCG AGA	5'- GGT GAG CCT GTA TTG GGA CAA
Nestin	5'- CTG CAG GCC ACT GAA AAG TT	5'- GAC CCT GCT TCT CCT GCT C
Kir4.1	5'- GCA GGT GAA TGC GAT GGC TA	5'- CAG AAT GAA GTG AAG CCC AGG
Tuj-1	5'- CTA GCC GCG TGA AGT CAG CA	5'- CCA AAG GCG CCA GAC CGA ACA
GAPDH	5'- GCC TTC CGT GTT CCT ACC	5'- CCT CAG TGT AGC CCA AGA TG

GFAP, glial fibrillary acidic protein.

RESULTS

Colocalization of Kir4.1, Sox2, and Nestin in activated astrocytes in the injured brain

Both Western blotting and immunostaining showed that levels of Kir4.1 were quite low in the intact brain (Fig. 1A, B). To examine the expression of Kir4.1 in the injured brain, we induced brain injury by injecting ATP, a component of damage-associated molecular patterns (DAMP), into the striatum of mouse brains as previously reported [22,27,28]. At 3 and 7 d post-injury, levels of Kir4.1 protein as well as those of GFAP, a marker of reactive astrocytes, were significantly increased (Fig. 1A). Immunostaining also showed increased Kir4.1 expression near the damage core (*) at 3 and 7 d, and decreased at 14 d (Fig. 1B). We further found that GFAP-positive cells in the penumbra region adjacent to the damage core highly expressed Kir4.1 at 3 d (Fig. 1Ca, arrows) and 7 d (Fig. 1Cc, arrows) post-injury, with Kir4.1 staining intensity

increasing with increased proximity to the damage core (Fig. 1Ca vs. Cb; Fig. 1Cc vs. Cd).

In the ATP-injured brain, Kir4.1 showed colocalization with Nestin (Fig. 1Ca–d), a marker of stem cells [29,30]. Kir4.1/GFAP/Nestin immunostaining showed that GFAP and Nestin exhibited the same pattern of expression following damage as that shown for Kir4.1 in Fig. 1B. GFAP and Nestin levels, like those of Kir4.1, were quite low or undetectable in the intact brain, as shown by Western blotting (Fig. 1C vs. Fig. 1A). Interestingly, Nestin was detectable in astrocytes that highly expressed Kir4.1 (Fig. 1C). Sox2, another stem cell marker [20], was also detectable at 3 and 7 d post injury at enhanced levels compared with its low expression in the intact brain (Fig. 1D vs. Fig. 1A). In the penumbra region adjacent to the damage core, Sox2 expression was highly increased in Kir4.1- and GFAP-positive cells (Fig. 1Da–d, arrows). In addition, there were more Sox2-positive cells in penumbra regions closer to the core: at 3 d, about 80% of Sox2/GFAP-double positive cells were Kir4.1-positive in region a, but only ~40% of

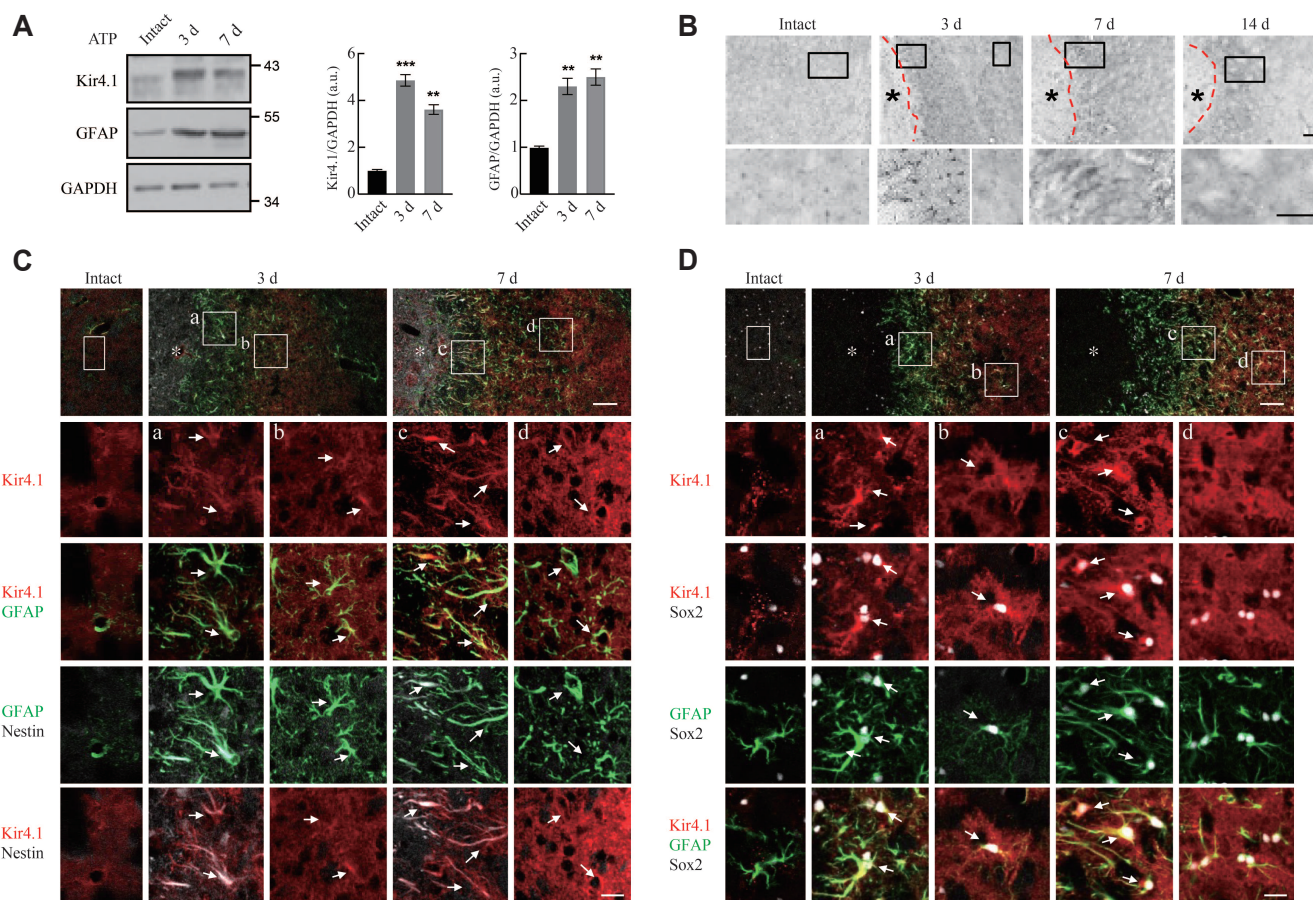


Fig. 1. Kir4.1 expression is increased in the injured brain. Brain damage was induced by stereotaxic injection of ATP (400 nM) into the striatum. (A) Proteins were prepared at the indicated times after ATP injection, and expression levels of Kir4.1 and glial fibrillary acidic protein (GFAP) were analyzed by Western blotting and quantified using Image J. GAPDH was used as a loading control. Values are presented as means \pm SEMs of three samples (** $p < 0.001$, *** $p < 0.0001$). (B–D) Brain sections were prepared at the indicated times after ATP injection and stained with antibodies for Kir4.1 (B), Kir4.1/Nestin/GFAP (C), or Kir4.1/Sox2/GFAP (D). Penumbra regions adjacent to the damage core (*) and farther from the core are designated (a, c) and (b, d), respectively. Scale bars: 100 μ m (B, C, and D, upper panel) and 20 μ m (C and D, lower panel).

such cells were Kir4.1-positive in region b (Fig. 1Da vs. Fig. 1Db). These results show that expression of both Kir4.1 and the stem cell markers Nestin and Sox2 are increased in reactive astrocytes near the damage core. Interestingly, Kir4.1 channels, which mediate K^+ efflux out of cells and thereby hyperpolarize the membrane potential [9,10], are reported to be involved in regulating the proliferation/differentiation of cells [9,10,31,32], consistent with reports that depolarization favors cell proliferation [33]. Collectively, these observations raise the question of whether Kir4.1 is involved in the gain of stemness and/or proliferation of astrocytes in the injured brain.

Kir4.1 expression and function in the acquisition of stemness

Next, we examined whether there is a linkage between Kir4.1 expression and the acquisition of stemness, demonstrated by the expression of Nestin and Sox2. For this, stem cells were cultured

from E13.5 or P7 mouse brains.

Stem cells from E13.5 mouse brains cultured in the presence of EGF (20 ng/ml) and FGF (20 ng/ml) formed neurospheres after 5 d in culture (Fig. 2A). During neurosphere formation, mRNA levels of Sox2, Nestin, GFAP, and Kir4.1 increased, whereas mRNA expression of β -tubulin III (Tubb3) was decreased (Fig. 2A). To examine the role of Kir4.1 channels in neurosphere formation, we cultured neurospheres in the presence of the Kir4.1 blocker, BaCl₂ (Fig. 2B). EGF/FGF increased sphere size at day 5, but BaCl₂ had little effect on the size of spheres with or without EGF/FGF (Fig. 2B). BaCl₂ likewise had little effect on Sox2, Nestin, Tubb3, or GFAP mRNA expression during neurosphere formation (Fig. 2C).

Next, we examined the effect of Kir4.1 inhibition on acquisition of stemness and expression of Nestin and Sox2 in stem cells prepared from P7 mouse brains. In the presence of EGF (20 ng/ml)/FGF (20 ng/ml), these stem cells, like those from E13.5 mouse brains, formed neurospheres after 5 d in culture (Fig.

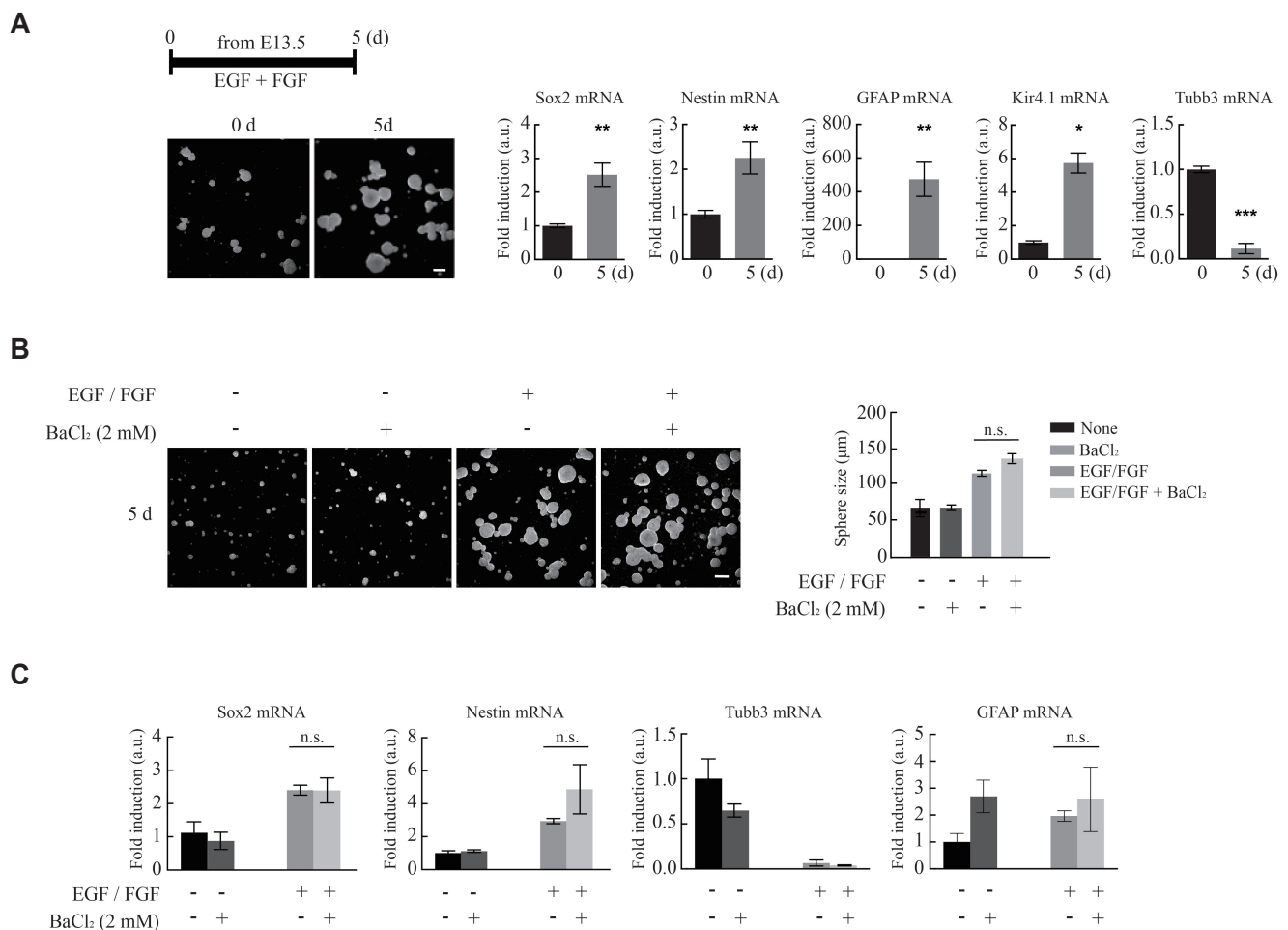


Fig. 2. The Kir4.1 blocker, BaCl₂, has little effect on self-renewal of stem cells or expression of Sox2 and Nestin. Cells from E13.5 mouse brains were cultured with epidermal growth factor (EGF) (20 ng/ml)/fibroblast growth factor (FGF) (20 ng/ml) and BaCl₂ as indicated. (A, B) Size of spheres was measured. Scale bars: 100 μm. (A, C) mRNA levels of the indicated factors were analyzed. Values are means ± SEMs of three samples (*p < 0.05, **p < 0.001, ***p < 0.0001).

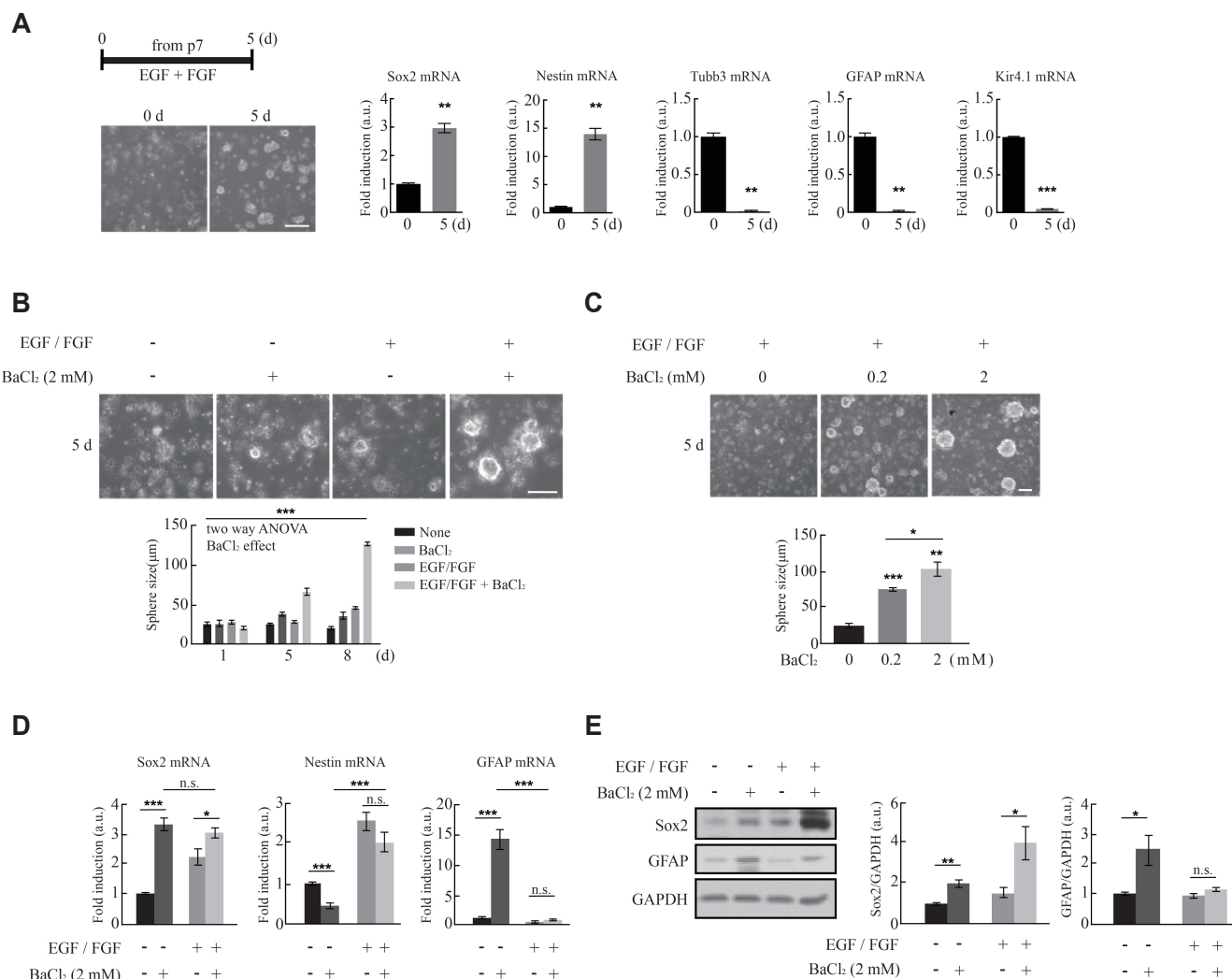


Fig. 3. BaCl₂ enhances self-renewal of stem cells and increases Sox2 expression. Cells from P7 mouse brains were cultured with epidermal growth factor (EGF)/fibroblast growth factor (FGF) and BaCl₂ as indicated. (A–C) Size of spheres was measured. Scale bars: 100 μ m. (A, D, E) mRNA (A, D) and protein (E) levels of the indicated factors were analyzed. GAPDH was used as a loading control (D). Values are means \pm SEMs of three samples (* p < 0.05, ** p < 0.001, *** p < 0.0001).

3A). During neurosphere formation, mRNA levels of Sox2 and Nestin increased, whereas those of GFAP and Tub3 decreased, as expected (Fig. 3A). Interestingly, in contrast to results obtained using stem cells from E13.5 mouse brains, mRNA levels of Kir4.1 decreased during formation of neurospheres from stem cells obtained from P7 mouse brains (Fig. 3A). To examine the role of Kir4.1 in neurosphere formation, we cultured neurospheres in the presence of BaCl₂, with and without EGF/FGF (Fig. 3B). In the presence of EGF/FGF, BaCl₂ significantly increased the size of spheres at day 5, an effect that became more obvious at day 8 (Fig. 3B). BaCl₂ also caused a concentration-dependent increase in sphere size in the presence of EGF/FGF (Fig. 3C). Even in the absence of EGF/FGF, BaCl₂ alone slightly increased sphere size (Fig. 3B). These loss-of-function results suggest that, under normal conditions, Kir4.1 may negatively regulate the proliferation of cells during neurosphere formation.

Next, we examined the effect of Kir4.1 inhibition on Sox2 and Nestin expression during neurosphere formation. BaCl₂ alone significantly elevated Sox2 expression at both mRNA (Fig. 3D) and protein levels (Fig. 3E), and potentiated EGF/FGF-induced Sox2 protein expression (Fig. 3E). Interestingly, the EGF/FGF-induced increase in Sox2 mRNA was not greater than that induced by BaCl₂ alone (Fig. 3D). In contrast, BaCl₂ alone slightly reduced Nestin mRNA levels and had little effect on EGF/FGF-induced Nestin mRNA expression (Fig. 3D). BaCl₂ significantly enhanced both mRNA and protein levels of GFAP (Fig. 3D, E) and had little effect on the EGF/FGF-induced reduction in GFAP mRNA and protein levels (Fig. 3D, E). Taken together, these results suggest that blocking Kir4.1 in P7 stem cells favors neurosphere formation and expression of Sox2 and GFAP, but has little effect on Nestin expression.

Kir4.1 expression and role in differentiation of neural stem cells

Finally, we examined the effect of Kir4.1 on the differentiation of stem cells. For this, we induced differentiation of stem cells prepared from E13.5 mouse brains by withdrawal of EGF and FGF

in the culture medium, and then measured levels of Sox2, Nestin, GFAP, and Tubb3. During differentiation of neural stem cells (NSCs), mRNA and/or protein levels of Sox2 and Nestin were decreased, whereas those of GFAP and Tubb3 increased (Fig. 4A, B). Kir4.1 expression was significantly increased at both mRNA and protein levels at 1 d; its expression decreased at 3 and 5 d, but was

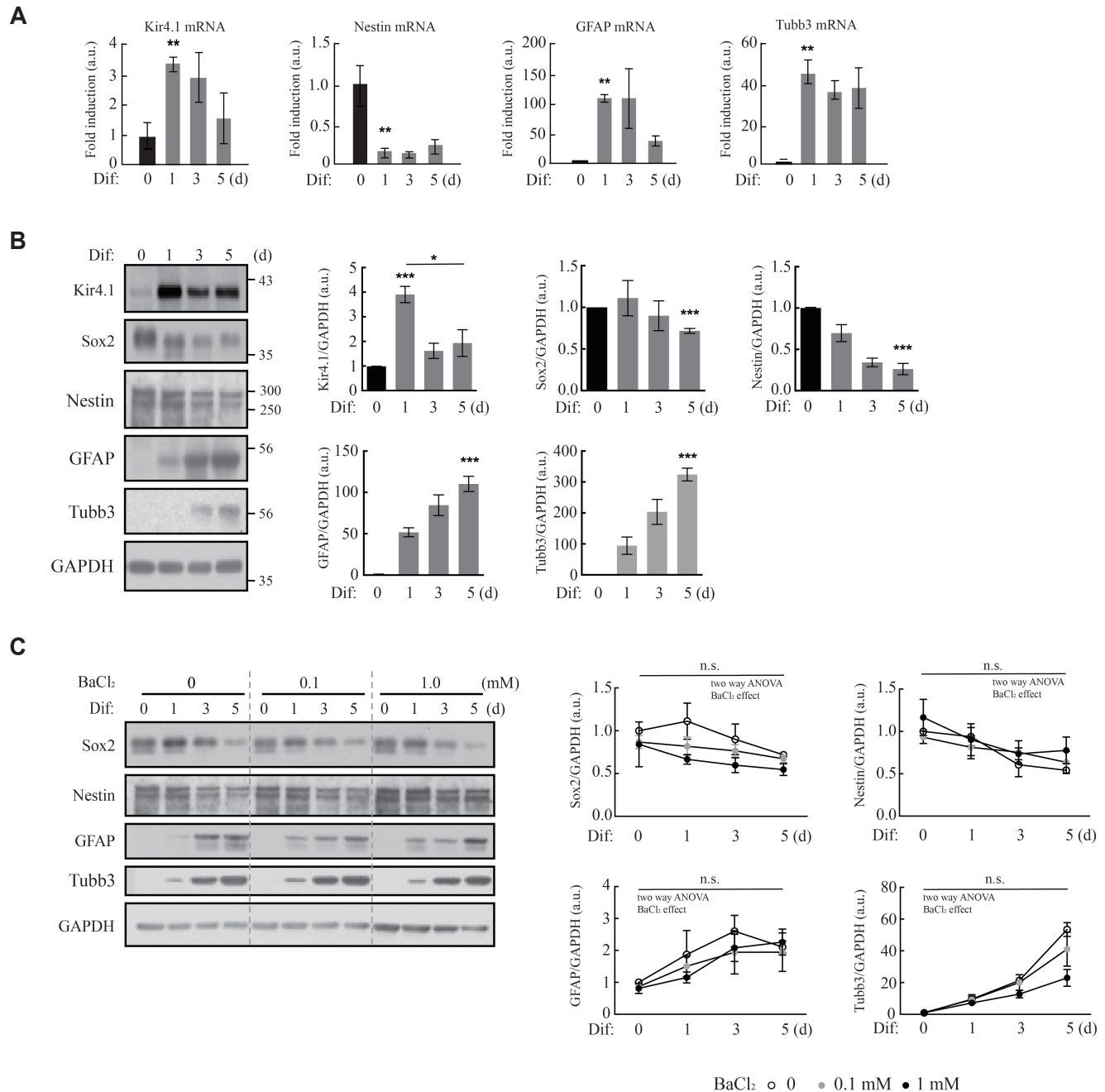


Fig. 4. Kir4.1 expression and effect of Kir4.1 inhibition on differentiation of neural stem cells. NSCs were prepared from E13.5 mouse embryo brains and cultured with or without BaCl₂. Differentiation was induced by withdrawal of epidermal growth factor (EGF) and fibroblast growth factor (FGF) from the culture medium. (A) mRNA levels of Nestin, glial fibrillary acidic protein (GFAP), Tubb3, and Kir4.1 at the indicated times after induction of differentiation were analyzed using qPCR. au, arbitrary unit. (B, C) Protein levels of Sox2, Nestin, GFAP, Tubb3 (Tuj-1 antibody), and Kir4.1 were analyzed by Western blotting (left panel) and quantified using Image J (right panel). GAPDH was used as a loading control. Values are means ± SEMs of three samples (**p* < 0.05, ***p* < 0.001, ****p* < 0.0001).

still maintained above basal levels (Fig. 4A, B). Treatment of NSCs with BaCl₂ during differentiation caused little change in expression levels of Sox2, Nestin, GFAP or Tubb3 (Fig. 4C). Collectively, these results suggest that Kir4.1 does not regulate differentiation (i.e., loss of stemness) of stem cells.

DISCUSSION

The results of this study showed that, in injured brains, Kir4.1 is highly expressed in reactive astrocytes that possess stem cell properties, as evidenced by expression of Nestin and Sox2. Treatment with the Kir4.1 blocker, BaCl₂, increased Sox2 expression and the size of neurospheres formed from stem cells cultured from P7 mouse brains, but had little effect on the differentiation of stem cells. Accordingly, Kir4.1 may play a role in negatively regulating the acquisition of stemness, although the possibility that effects of BaCl₂ apart from Kir4.1 channel block might have increased Sox2 expression and size of neurospheres cannot be ruled out.

It has been reported that reactive astrocytes have stem cell-like properties, and as such express the stem cell markers, Nestin and Sox2 [20,29,30]. We found that Kir4.1 expression was upregulated together with Sox2 and Nestin in reactive astrocytes in the penumbra region of the injured brain (Fig. 1). In spheres formed from stem cells in the presence of EGF/FGF, Kir4.1 expression showed opposite patterns depending on the age of mouse brains: it increased in stem cells obtained from E13.5 mouse brains, but decreased in P7 stem cells (Fig. 2 vs. Fig. 3). The effect of Kir4.1 inhibition with BaCl₂ was also different: it had little effect on Sox2 expression and sphere size in stem cells from E13.5 mouse brains, but increased both in P7 stem cells (Fig. 2 vs. Fig. 3). Thus, blocking Kir4.1 expression in the initial stage of sphere formation in P7 stem cells may be sufficient to increase the self-renewal of stem cells.

BaCl₂-mediated Kir4.1 inhibition had less of an effect on Nestin levels than Sox2 levels in P7 stem cells (Fig. 3), suggesting that Sox2 may be more important for self-renewal of stem cells relative to Nestin. Though used as a stem cell marker, Nestin is a cytoskeletal protein that increases during cell division [34]. By contrast, Sox2, a key transcription factor, regulates the expression of genes required for the pluripotency of stem cells, and its expression is down-regulated during differentiation [35]. Consistent with this, it has been reported that Sox2 plays important roles in brain development and shows increased expression in neural progenitor cells in the injured spinal cord [21,36]. Cytoskeletal proteins, including Nestin, could be increased as a result of proliferation, a characteristic property of reactive astrocytes. Kir4.1 expression was significantly increased at an early stage during NSC differentiation (Fig. 4). However, Kir4.1 may not play important roles in differentiation, given that BaCl₂ had little effect on expression levels of Sox2 or those of GFAP and Tubb3 during NSC differen-

tiation (Fig. 4). Taken together, these results suggest that Kir4.1 plays a role during the acquisition phase of stemness but has little involvement in the loss of stemness.

Studies on Kir4.1 have focused on its functions as an ion channel, such as regulation of membrane potential and maintaining extracellular K⁺ homeostasis [1-3]. Therefore, whether and how Kir4.1 regulates stemness is largely unknown. During sphere formation, Kir4.1 mRNA levels were decreased in association with an increase in Sox2 expression (Fig. 3), and inhibition of Kir4.1 function with BaCl₂ upregulated Sox2 expression and induced a concentration-dependent increase in sphere size (Fig. 3). BaCl₂ blocks Kir4.1-mediated K⁺ efflux and increases intracellular K⁺ ions, thereby depolarizing the membrane potential [10]. Depolarization, in turn, activates voltage-gated Ca²⁺ channels, which mediate influx of extracellular Ca²⁺ ions; the resulting increase in intracellular Ca²⁺ ions activate several downstream signaling pathways that may regulate cell proliferation [9,10,37]. In future studies, it will be necessary to investigate whether increased Sox2 expression is related to increases in intracellular Ca²⁺ using Ca²⁺ chelators, such as EDTA or EGTA.

In conclusion, endogenous brain stem cells are considered critical targets in the treatment of a broad spectrum of diseases, including ischemia and neurodegenerative diseases [14,16,38]. However, despite accumulating evidence showing that the number of cells with stem cell properties is increased in the injured brain, it is not yet clear how stemness is acquired and regulated in the injured brain. The results of this study revealed that upregulated Kir4.1 in reactive astrocytes may act as a regulator to finely control the extent of stemness of these cells by inhibiting the expression of Sox2. Therefore, Kir4.1 may be an important target for modulating stemness during cellular remodeling in the injured brain.

ACKNOWLEDGEMENTS

This work was supported by grants funded by the Korean government (NRF-2017R1A2B3011281 and NRF-2016M3C7A1905072), and a grant from KOSEF through the Chronic Inflammatory Disease Research Center at Ajou University (NRF-2012R1A5A048183) to EJ.

CONFLICTS OF INTEREST

The authors declare no conflicts of interest.

REFERENCES

1. Kofuji P, Ceelen P, Zahs KR, Surbeck LW, Lester HA, Newman EA. Genetic inactivation of an inwardly rectifying potassium channel

- (Kir4.1 subunit) in mice: phenotypic impact in retina. *J Neurosci*. 2000;20:5733-5740.
2. Poopalasundaram S, Knott C, Shamotienko OG, Foran PG, Dolly JO, Ghiani CA, Gallo V, Wilkin GP. Glial heterogeneity in expression of the inwardly rectifying K⁺ channel, Kir4.1, in adult rat CNS. *Glia*. 2000;30:362-372.
 3. Yakushigawa H, Tokunaga Y, Inanobe A, Kani K, Kurachi Y, Maeda T. A novel junction-like membrane complex in the optic nerve astrocyte of the Japanese macaque with a possible relation to a potassium ion channel. *Anat Rec*. 1998;250:465-474.
 4. Nagelhus EA, Mathiisen TM, Ottersen OP. Aquaporin-4 in the central nervous system: cellular and subcellular distribution and coexpression with KIR4.1. *Neuroscience*. 2004;129:905-913.
 5. Djukic B, Casper KB, Philpot BD, Chin LS, McCarthy KD. Conditional knock-out of Kir4.1 leads to glial membrane depolarization, inhibition of potassium and glutamate uptake, and enhanced short-term synaptic potentiation. *J Neurosci*. 2007;27:11354-11365.
 6. Cui Y, Yang Y, Ni Z, Dong Y, Cai G, Foncelle A, Ma S, Sang K, Tang S, Li Y, Shen Y, Berry H, Wu S, Hu H. Astroglial Kir4.1 in the lateral habenula drives neuronal bursts in depression. *Nature*. 2018;554:323-327.
 7. Tong X, Ao Y, Faas GC, Nwaobi SE, Xu J, Hausteine MD, Anderson MA, Mody I, Olsen ML, Sofroniew MV, Khakh BS. Astrocyte Kir4.1 ion channel deficits contribute to neuronal dysfunction in Huntington's disease model mice. *Nat Neurosci*. 2014;17:694-703.
 8. Srivastava R, Aslam M, Kalluri SR, Schirmer L, Buck D, Tackenberg B, Rothhammer V, Chan A, Gold R, Berthele A, Bennett JL, Korn T, Hemmer B. Potassium channel KIR4.1 as an immune target in multiple sclerosis. *N Engl J Med*. 2012;367:115-123.
 9. Urrego D, Tomczak AP, Zahed F, Stühmer W, Pardo LA. Potassium channels in cell cycle and cell proliferation. *Philos Trans R Soc Lond B Biol Sci*. 2014;369:20130094.
 10. Yasuda T, Bartlett PF, Adams DJ. K_{ir} and K_v channels regulate electrical properties and proliferation of adult neural precursor cells. *Mol Cell Neurosci*. 2008;37:284-297.
 11. Pekny M, Nilsson M. Astrocyte activation and reactive gliosis. *Glia*. 2005;50:427-434.
 12. Eng LF, Ghirmikar RS. GFAP and astrogliosis. *Brain Pathol*. 1994;4:229-237.
 13. Kernie SG, Erwin TM, Parada LF. Brain remodeling due to neuronal and astrocytic proliferation after controlled cortical injury in mice. *J Neurosci Res*. 2001;66:317-326.
 14. Duan CL, Liu CW, Shen SW, Yu Z, Mo JL, Chen XH, Sun FY. Striatal astrocytes transdifferentiate into functional mature neurons following ischemic brain injury. *Glia*. 2015;63:1660-1670.
 15. Götz M, Sirko S, Beckers J, Irmeler M. Reactive astrocytes as neural stem or progenitor cells: in vivo lineage, in vitro potential, and genome-wide expression analysis. *Glia*. 2015;63:1452-1468.
 16. Magnusson JP, Göritz C, Tatarishvili J, Dias DO, Smith EM, Lindvall O, Kokaia Z, Frisén J. A latent neurogenic program in astrocytes regulated by Notch signaling in the mouse. *Science*. 2014;346:237-241.
 17. Sirko S, Behrendt G, Johansson PA, Tripathi P, Costa M, Bek S, Heinrich C, Tiedt S, Colak D, Dichgans M, Fischer IR, Plesnila N, Staufenbiel M, Haass C, Snapyan M, Saghatelian A, Tsai LH, Fischer A, Grobe K, Dimou L, et al. Reactive glia in the injured brain acquire stem cell properties in response to sonic hedgehog. [corrected]. *Cell Stem Cell*. 2013;12:426-439.
 18. Shimada IS, LeComte MD, Granger JC, Quinlan NJ, Spees JL. Self-renewal and differentiation of reactive astrocyte-derived neural stem/progenitor cells isolated from the cortical peri-infarct area after stroke. *J Neurosci*. 2012;32:7926-7940.
 19. Buffo A, Rite I, Tripathi P, Lepier A, Colak D, Horn AP, Mori T, Götz M. Origin and progeny of reactive gliosis: a source of multipotent cells in the injured brain. *Proc Natl Acad Sci U S A*. 2008;105:3581-3586.
 20. Zappone MV, Galli R, Catena R, Meani N, De Biasi S, Mattei E, Tiveron C, Vescovi AL, Lovell-Badge R, Ottolenghi S, Nicolis SK. Sox2 regulatory sequences direct expression of a (beta)-geo transgene to telencephalic neural stem cells and precursors of the mouse embryo, revealing regionalization of gene expression in CNS stem cells. *Development*. 2000;127:2367-2382.
 21. Bani-Yaghoob M, Tremblay RG, Lei JX, Zhang D, Zurakowski B, Sandhu JK, Smith B, Ribocco-Lutkiewicz M, Kennedy J, Walker PR, Sikorska M. Role of Sox2 in the development of the mouse neocortex. *Dev Biol*. 2006;295:52-66.
 22. Grazioli S, Pugin J. Mitochondrial damage-associated molecular patterns: from inflammatory signaling to human diseases. *Front Immunol*. 2018;9:832.
 23. Schaefer L. Complexity of danger: the diverse nature of damage-associated molecular patterns. *J Biol Chem*. 2014;289:35237-35245.
 24. Le Feuvre RA, Brough D, Touzani O, Rothwell NJ. Role of P2X7 receptors in ischemic and excitotoxic brain injury in vivo. *J Cereb Blood Flow Metab*. 2003;23:381-384.
 25. Zheng LM, Zychlinsky A, Liu CC, Ojcius DM, Young JD. Extracellular ATP as a trigger for apoptosis or programmed cell death. *J Cell Biol*. 1991;112:279-288.
 26. Yang H, An J, Choi I, Lee K, Park SM, Jou I, Joe EH. Region-specific astrogliosis: differential vessel formation contributes to different patterns of astrogliosis in the cortex and striatum. *Mol Brain*. 2020;13:103.
 27. Jeong HK, Ji KM, Min KJ, Choi I, Choi DJ, Jou I, Joe EH. Astrogliosis is a possible player in preventing delayed neuronal death. *Mol Cells*. 2014;37:345-355.
 28. Jeong HK, Ji KM, Kim B, Kim J, Jou I, Joe EH. Inflammatory responses are not sufficient to cause delayed neuronal death in ATP-induced acute brain injury. *PLoS One*. 2010;5:e13756.
 29. Suzuki S, Namiki J, Shibata S, Mastuzaki Y, Okano H. The neural stem/progenitor cell marker nestin is expressed in proliferative endothelial cells, but not in mature vasculature. *J Histochem Cytochem*. 2010;58:721-730.
 30. Lendahl U, Zimmerman LB, McKay RD. CNS stem cells express a new class of intermediate filament protein. *Cell*. 1990;60:585-595.
 31. Olsen ML, Sontheimer H. Functional implications for Kir4.1 channels in glial biology: from K⁺ buffering to cell differentiation. *J Neurochem*. 2008;107:589-601.
 32. Higashimori H, Sontheimer H. Role of Kir4.1 channels in growth control of glia. *Glia*. 2007;55:1668-1679.
 33. Lan JY, Williams C, Levin M, Black LD 3rd. Depolarization of cellular resting membrane potential promotes neonatal cardiomyocyte proliferation in vitro. *Cell Mol Bioeng*. 2014;7:432-445.
 34. Frederiksen K, McKay RD. Proliferation and differentiation of rat neuroepithelial precursor cells in vivo. *J Neurosci*. 1988;8:1144-1151.
 35. Avilion AA, Nicolis SK, Pevny LH, Perez L, Vivian N, Lovell-Badge

- R. Multipotent cell lineages in early mouse development depend on SOX2 function. *Genes Dev.* 2003;17:126-140.
36. Goldshmit Y, Frisca F, Pinto AR, Pébay A, Tang JK, Siegel AL, Kaslin J, Currie PD. Fgf2 improves functional recovery-decreasing gliosis and increasing radial glia and neural progenitor cells after spinal cord injury. *Brain Behav.* 2014;4:187-200.
37. Catterall WA. Voltage-gated calcium channels. *Cold Spring Harb Perspect Biol.* 2011;3:a003947.
38. Man JHK, Groenink L, Caiazzo M. Cell reprogramming approaches in gene- and cell-based therapies for Parkinson's disease. *J Control Release.* 2018;286:114-124.